Astrocyte glucocorticoid signaling mediates cognitive impairment induced by early-life stress

Authors: Ifeoluwa I. Adedipe[1,2,*], Lewis R. Depaauw-Holt[1,2,*], Jade Latraverse-Arquilla[2], Juliette Vaugeois[1,2], Manon Duquenne[1,2], Benjamin Rogers[1,2], Sarah Peyrard[2], Anthony Bosson[2] and Ciaran Murphy-Royal[1,2,‡].

Affiliations:

1. Département de Neurosciences, Université de Montréal, Montréal, Québec, Canada.
2. Centre de Recherche du Centre Hospitalier de l'Université de Montréal (CRCHUM), Montréal, Québec, Canada

* Co-first authors

‡ Corresponding author

Corresponding author: Ciaran Murphy-Royal (ciaran.murphy-royal@umontreal.ca)
CRCHUM, 900 rue st Denis, Montéal, Québec, Canada, H2X 0A9

Abstract:

Early-life stress can have lifelong consequences, enhancing stress susceptibility and resulting in behavioural and cognitive deficits. While the effects of early-life stress (ELS) on neuronal function have been well-described, we still know very little about the contribution of non-neuronal brain cells to the cellular and behavioural adaptations following ELS. Here, using a rodent model of ELS, we report that astrocytes play a key role in mediating the impact of stress on amygdala-dependent behaviour and synaptic plasticity during adolescence. We report that ELS induces generalisation of fear, associated with increased levels of circulating corticosterone and activation of glucocorticoid receptors in astrocytes. In addition, we identify astrocyte glucocorticoid receptors as targets, mediating ELS-induced cognitive and synaptic impairments. This work establishes astrocytes as key elements in amygdala-dependent memory, and as central mediators of the effects of stress on cognitive function via stress hormone signalling pathways.

Summary:

1. ELS impairs lateral amygdala-dependent cognition and synaptic plasticity during adolescence.

2. Stress-induced behavioural changes were associated with astrocyte dysfunction in the lateral amygdala.

3. Genetic disruption of astrocyte function in the lateral amygdala replicated the cognitive and synaptic impairments induced by stress.

4. ELS induced a latent increase in blood glucocorticoid levels during adolescence.

5. Ablating glucocorticoid signalling in astrocytes rescued cognitive impairments induced by ELS.

Introduction:

Both human and rodent studies have provided compelling evidence for the long-lasting effects of adverse early-life experiences, highlighting enhanced susceptibility to subsequent stressors later in life[1–5]. ELS has widespread effects across the brain and can influence many neural circuits including those involved in threat detection, emotion, cognitive processing, and reward seeking behaviors[6–10]. Research in this domain has predominantly focused upon investigating the effects of stress on neuronal cells and the consequences for behaviour[11–14]. We have gleaned tremendous insight into disorders of stress from these studies, yet the links between stress, brain circuits and behaviour remain tenuous. Within this framework, the contribution of distinct brain cells, including astrocytes, remains largely untested. Glial cells, which comprise approximately half the cell population in the brain have been shown to directly regulate synaptic transmission and plasticity[15–19], thereby influencing many discrete behaviours[20–30]. Despite the abundance of research suggesting important roles for astrocytes in regulating affective states[31], fear[32], and reward seeking behaviors[20,33], whether astrocyte dysfunction prompts stress-induced behavioral impairments remains unknown.

To answer this question we performed behavioural tests targeting the lateral amygdala, a brain region involved with threat detection and associative learning that is acutely sensitive to stress[14,34–39]. Using auditory discriminative fear conditioning, an amygdala-dependent behavioural task[40–42], we find that ELS impairs discrimination of neutral from aversive auditory cues. This was associated with impaired synaptic plasticity in cortico-amygdala circuits, recorded in acute brain slices. We characterised the impact of ELS on astrocytes in the lateral amygdala revealing changes in specific proteins associated morphological reorganisation and astrocyte network function. Genetic disruption of astrocyte function, specifically in the lateral amygdala, recapitulated ELS-induced behavioural and synaptic phenotypes, supporting the hypothesis that astrocytes strongly contribute to the impact of stress on neural circuits. Finally, we reveal that attenuating glucocorticoid signalling in lateral amygdala astrocytes fully rescued the impact of ELS on cognition, with a marked improvement in auditory discrimination. Together, these findings identify astrocytes as key elements regulating amygdala-dependent affective memory and highlight astrocytes as central mediators of the long-term impact of stress on amygdala circuit function.

Results:

1. Early-life stress impairs lateral amygdala-dependent memory and synaptic plasticity

We employed an ELS paradigm which combines limited bedding and nesting materials, as well as maternal separation from postnatal days 10 to 17 (**Fig. 1a**). This ELS paradigm has been shown to induce life-long stress susceptibility and affect reward circuitry[6]. Furthermore, this paradigm aligns with a critical neurodevelopmental window during which astrocytes mature and integrate with synapses[43,44]. As such, any perturbation of astrocytes during this critical period has the potential to disrupt numerous roles of these cells in neural function.

We first characterised the impact of this stress paradigm on lateral amygdala-dependent learning and memory using auditory discriminative fear conditioning. In brief, during this paradigm mice are exposed to a neutral auditory cue (conditioned stimulus -; CS-) and an aversive cue (CS+) paired with footshock (unconditioned stimulus; US; **Fig. 1b**). On day two mice are placed in a novel environment and each auditory cue is played with freezing (immobility) quantified as a measure of learning and memory (**Fig. 1c**). Mice accurately learn this task and can readily distinguish between naïve and aversive cues (**Suppl. Fig. 1a-c**). This learning and memory paradigm has been demonstrated to recruit the lateral amygdala and requires long-term potentiation in this brain region pairing input from auditory and somatosensory cortices[40].

Using naïve and ELS mice our data suggest that learning of CS+/US pairing is unaffected by ELS ($F_{(1,192)}$=2.999 p=0.08; naïve=37.51±8.4% N=20; ELS=41.67±6.7%, N=17; mean±s.e.m.) with a reduction in freezing to CS- in ELS group compared to naive ($F_{(1,186)}$=12.14 p=0.001; naïve=22.9±4.5%, N=20; ELS=13.55±3.5%, N=17; mean±s.e.m.; **Fig. 1d**). Memory recall was more subtly affected by ELS with no difference in freezing to CS+ ($F_{(1,210)}$=0.02; p=0.9; Naïve=58.77±3.2%, N=20; ELS=58.34±2.2%, N=17; mean±s.e.m.), however we found a significant increase in freezing response to CS- ($F_{(1,210)}$=16.29; p=0.001; Naïve=32.9±1.4%, N=20; ELS=46.03±2.9%, N=17; mean±s.e.m.) indicating generalisation of fear evidenced and freezing to non-aversive cues (**Fig. 1e**). This observation is more clearly depicted using a discrimination index (DI; DI>0 reflects accurate discrimination, DI=0 no discrimination and DI<0 reflects a discrimination error i.e. higher freezing to the neutral tone

than aversive tone) highlighting a significant decrease in fear discrimination in ELS mice compared to naïve mice ($F_{(1,210)}$=89.84, p=0.001; naïve=0.28±0.04; ELS=0.12±0.03; mean±s.e.m.; **Fig. 1f**). These data suggest that ELS impairs cognitive function *via* generalisation of fear, enhancing affective responses to neutral/non-aversive cues.

We observe no differences between male and female mice in this learning and memory paradigm with both sexes showing equal performance in learning (**Suppl. Fig. 1d**), and auditory discrimination (**Suppl. Fig. 1e,f**). We did, however, find a sex difference in the effect of ELS on cognitive function with a stronger impairment of ELS in female mice (**Suppl. Fig. 1g**).

Associative fear learning and memory paradigms, including the one employed in this study, have been correlated with synaptic changes in the lateral amygdala[40,45–47], to test whether we can observe similar synaptic changes associated with stress we carried out acute brain slice electrophysiology and recorded field excitatory postsynaptic potentials stimulating cortical inputs from the external capsule (**Fig. 1g**). We found that ELS results in decreased long-term potentiation of synaptic transmission (LTP) in response to theta burst stimulation (Naïve=164.5±27%, n=12; ELS=106±6.1%, n=13; mean±s.e.m; **Fig. 1h,i**). This synaptic observation is consistent with findings using distinct stress paradigms[15], and highlights the important influence of stress on synaptic function across various brain regions.

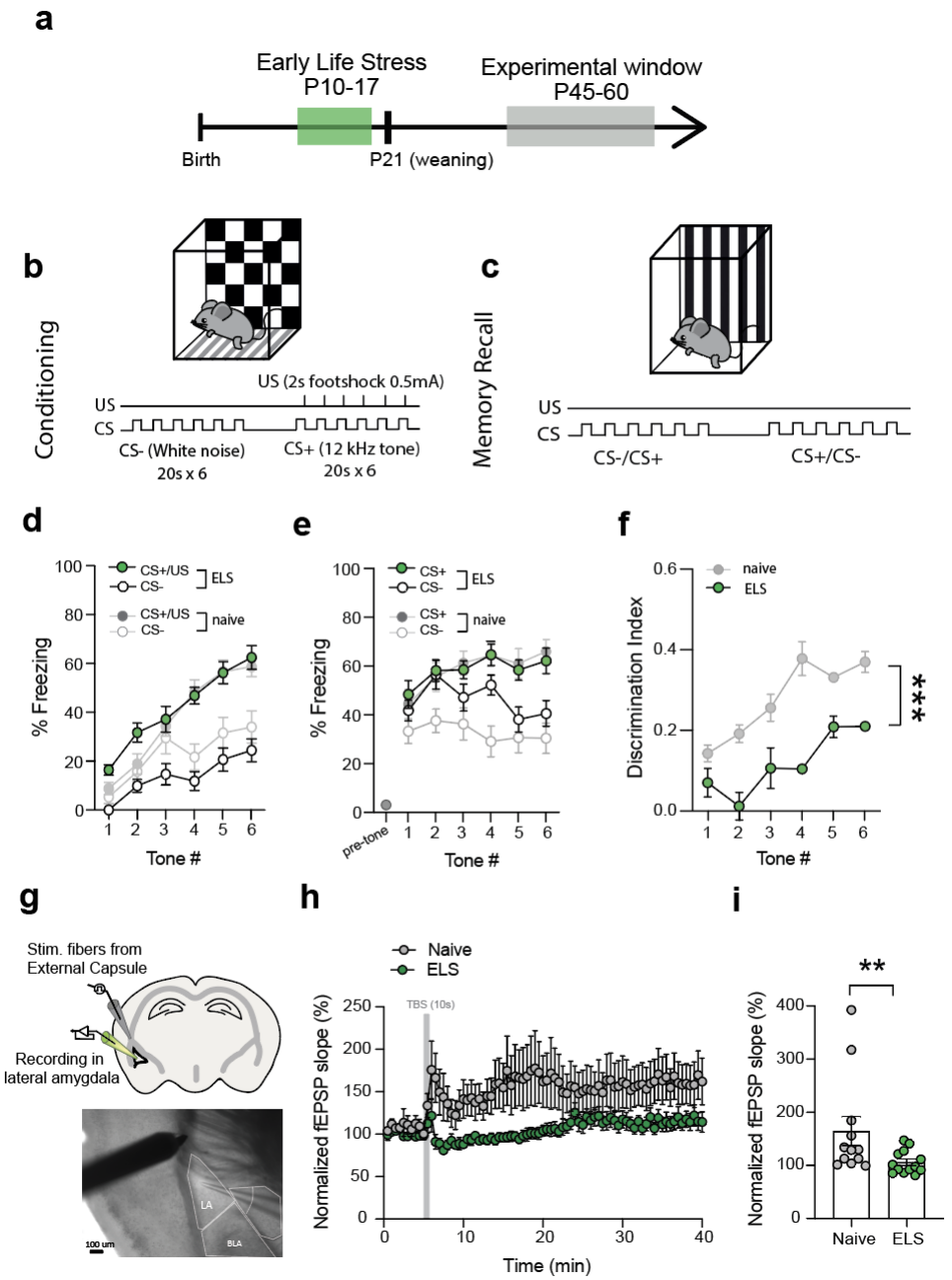

Figure 1. Effects of ELS on behaviour and synaptic function.
(a) Timeline of experimental paradigm. **(b)** Schematic representation of conditioning phase of auditory discriminative fear conditioning, and **(c)** memory recall phase. **(d)** Comparison of percentage of time spent freezing during CS+/US and CS- presentation during conditioning in ELS and naïve mice. **(e)** Comparison of percentage of time spent freezing during memory recall phase in ELS and naïve mice. **(f)** Comparison of discrimination between CS+ and CS- during memory recall phase in ELS and naïve mice. **(g)** *top* Schematic representation of electrophysiology stimulation and recording sites. *bottom* DIC image of stimulating and recording electrodes in an acute brain slice. **(h)** Average trace of field EPSP slope showing synaptic response to theta burst stimulation (*grey bar)* in naïve and ELS condition. **(i)** Bar chart comparing fEPSP slope at 30-40min post theta burst stimulation in naïve and ELS conditions.

2. Astrocytic response to early-life stress

To determine whether ELS impacts astrocytes in the lateral amygdala we carried out immunostaining on adolescent (P45-P60) stressed and naïve mice (**Fig. 2a,b**). We report a significant decrease in the cytoskeletal protein GFAP staining following ELS indicative of an astrocyte response (p=0.02, unpaired t-test; Naïve=1±0.17 a.u., n=11; ELS=0.5±0.1 a.u, n=12; mean±s.e.m.; **Fig. 2c**). To begin to determine functional outcomes we stained for astrocyte-specific proteins with known roles in influencing synaptic function including the gap-junction protein connexin 43 (Cx43) that contributes to astrocyte network function[48] and the glutamate transporter GLT-1, responsible for the efficient clearance of glutamate from the synaptic cleft[49]. Interestingly, we observed a decrease in fluorescence intensities only for Cx43 (p=0.008, unpaired t-test; Naïve=1±0.15 a.u., n=11; ELS=0.45±0.12 a.u., n=14; mean±s.e.m; **Fig. 2d**) while GLT-1 remained unaffected by stress (p=0.8, unpaired t-test; naïve=1±0.29 a.u., n=6; ELS=0.9±0.21 a.u., n=16; mean±s.e.m.; **Fig. 2e**). This suggests that astrocytes mount a specific response to stress, which could result in discrete changes astrocyte network function while leaving other functions such as neurotransmitter clearance unaffected.

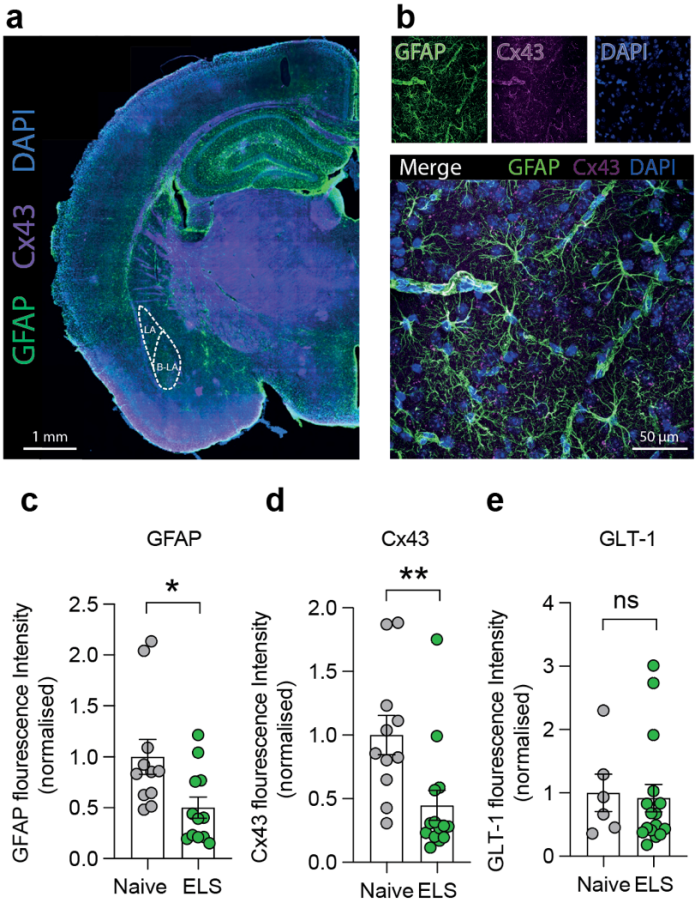

Figure 2. Impact of ELS on astrocytes. **(a)** Widefield image of GFAP, Cx43, and DAPI staining in the mouse brain, highlighting amygdala brain regions. **(b)** Confocal z-stack of the same image in the lateral amygdala. *top* single channel images of GFAP, Cx43, and DAPI with merge *below*. **(c)** Comparison of GFAP staining in naïve and ELS (normalised). **(d)** Comparison of Cx43 expression in naïve and ELS conditions (normalised). **(e)** Comparison of GLT-1 expression in naïve and ELS conditions (normalised).

3. Astrocyte dysfunction mirrors the effects of early-life stress

To directly implicate astrocytes in mediating the effects of ELS we carried out a series of genetic loss-of-function experiments, specifically targeting astrocytes in the lateral amygdala using a viral approach (**Fig. 3a**). Based on the putative astrocyte network dysfunction we identified (**Fig. 2d**), we first targeted astrocyte gap-junction coupling by overexpressing a dominant negative Cx43 (dnCx43). Second, to broadly target astrocyte function we used a calcium extruder pump (hPMCA2/b, a.k.a. CalEx) shown to clamp astrocyte calcium at minimal levels, effectively silencing these cells[22,50]. All viral constructs specifically targeted astrocytes with GfaABC1D promoter and were compared to a control virus expressing eGFP (**Fig. 3b**). Initially, we screened for behavioural changes in anxiety-like behaviors and report no impact of astrocyte specific manipulations on elevated plus maze (**Suppl. Fig. 2a-d**) and open field test (**Suppl. Fig. 2e-h**). These data show that viral injections alone do not produce innate behavioural impairment, and second that astrocytes in the lateral amygdala do not influence anxiety-like behaviour. Next, investigating the role of astrocytes in lateral amygdala-dependent cognitive processing, using auditory discriminative fear conditioning, we found that mice with impaired astrocyte network function (dnCx43 injected) displayed normal learning during the conditioning phase, i.e. more freezing to CS+/US pairing than CS- (**Fig. 3c**), and maintained some discrimination of neutral from aversive cues with greater freezing to CS+ than CS- ($F_{(1,192)}$=31.51, p=0.001; CS+=55.75±4.7%, CS-=38.59±2.2%; N=17 mean±s.e.m.; **Fig. 3d**). In mice where astrocyte calcium signalling was clamped with CalEx expression in the lateral amygdala, we observed intact learning as mice could differentiate CS+/US from CS- (**Fig. 3e**), but saw a clear impairment in cognitive function with no difference in freezing responses between CS+ and CS- ($F_{(1,120)=}$1.1, p=0.29; CS+=57.02±4.2%, CS-=53.0±1.2%; N=11; mean±s.e.m.; **Fig. 3f**). Quantification of cognitive impairment comparing the discrimination index revealed a decrease in fear discrimination in both dnCx43 and CalEx conditions, compared to viral control ($F_{(2,222)}$=141.5, p=0.001; Viral control DI=0.36±0.02, N=17; dnCx43 DI=0.17±0.04, N=17; CalEx DI=0.03±0.05, N=11; mean±s.e.m.; **Fig. 3g**). Fear discrimination was more severely impaired by CalEx than dnCx43, presumably due to the vast number of astrocyte intracellular processes that are potentially affected by this broad attenuation of intracellular calcium levels, that could include gliotransmitter release, intracellular signalling

cascades, and many other processes. Manipulation of astrocyte network function alone, which was identified as a target of ELS, more closely resembled the effects of stress than CalEx, supporting a specific astrocyte response to stress. Interestingly, these genetic manipulations of astrocyte function resulted in sex-specific behavioural responses with dnCx43 having a greater impact on male mice (**Suppl. Fig. 2j**) and CalEx impacting predominantly female mice (**Suppl. Fig. 2k**). These unexpected sex differences suggest sexual dimorphism in astrocyte mechanisms that influence behaviour.

To determine whether astrocyte function is also necessary for synaptic plasticity in the lateral amygdala, we carried out the same genetic manipulations and report that LTP is completely occluded by both astrocyte network dysfunction (p=0.02 - Control *vs.* dnCx43) or reduction in astrocyte calcium signalling (p=0.04 – Control *vs.* CalEx; Control (eGFP)=139±17.7%, n=5; dnCx43=98.31±8.64%, n=16; CalEx=100.3±7.5%; n=9; mean±s.e.m **; Fig. 3h,i**). Together these data highlight that astrocytes regulate synaptic plasticity and maintain proper cognitive function in this brain region.

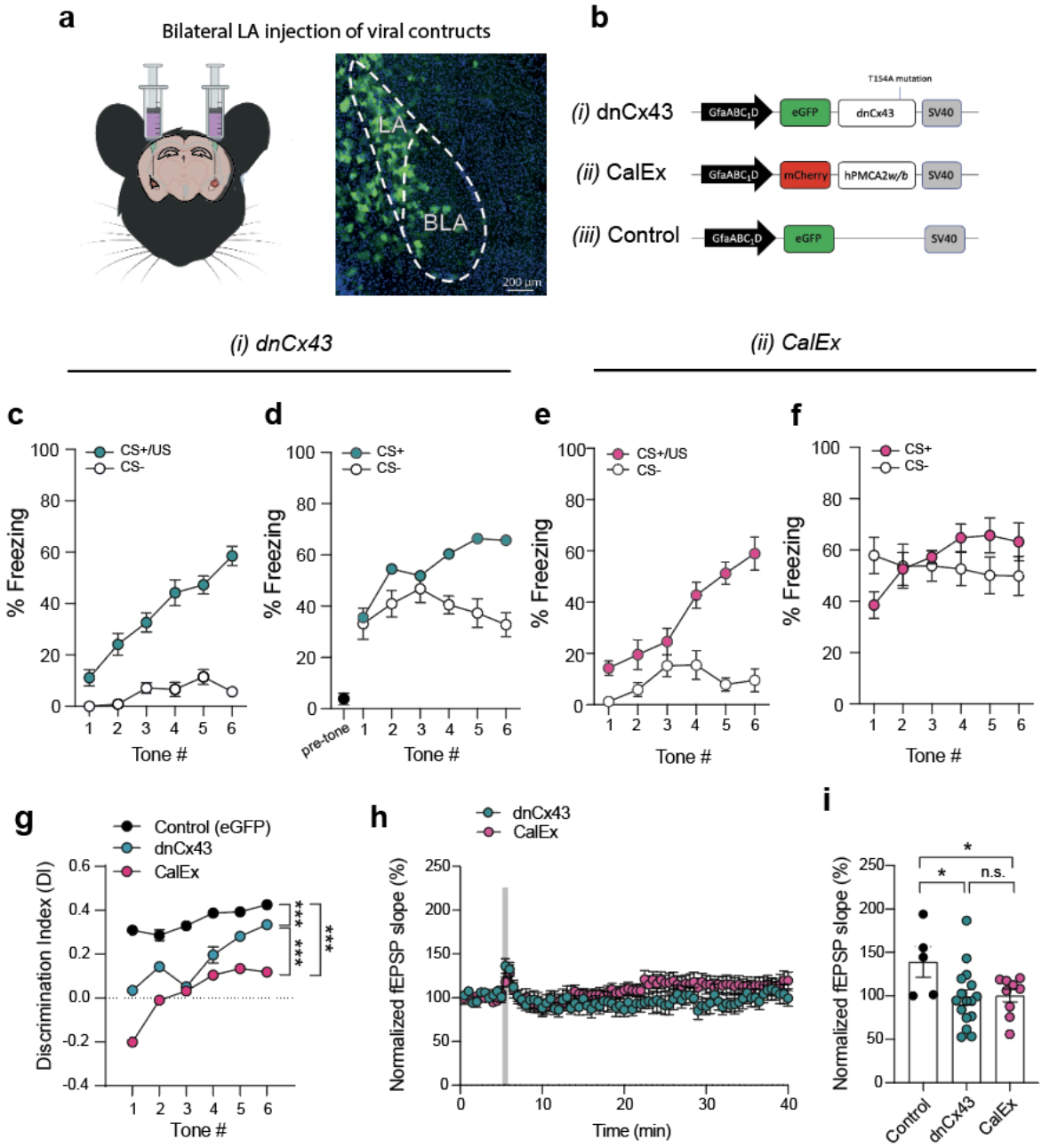

Figure 3. Astrocyte dysfunction alone mirrors effects of ELS on behaviour and synapses. **(a)** ***left*** Schematic representation of bilateral injection of AAVs targeting astrocyte function. ***right*** Example of fluorescent reporter expression in the lateral amygdala following AAV injection. **(b)** Three constructs were independently injected into LA to target astrocytes, (i) dnCx43, (ii) CalEx, and (ii) control virus. **(c)** Performance of dnCx43 injected mice during acquisition phase. **(d)** memory recall in dnCx43 injected mice. **(e)** Performance of CalEx injected mice in acquisition phase. **(f)** Memory recall in CalEx mice. **(g)** Comparison of discrimination index between dnCx43, CalEx, and Viral control. **(h)** Normalised fEPSP slope over the course of LTP experiment in dnCx43 and CalEx conditions. **(i)** Bar chart comparing fEPSP slope at 30-40min post theta burst stimulation in Control (eGFP), dnCx43, and CalEx injected conditions.

4. Early-life stress induced delayed increase in circulating glucocorticoids

The specific mechanism by which ELS affects astrocytes remains unknown. Considering previous work revealing that glucocorticoids influence astrocyte gene expression and function[15,51,52], we set out to determine whether this ELS paradigm might raise stress hormone levels. Taking trunk blood from mice across several litters at different time points in the ELS paradigm; pre-stress (P10), end of ELS paradigm (P17), and at the start of our experimental window (P45) and following our experimental window (P70; **Fig. 4a**), we report that this ELS paradigm induces a latent increase in blood CORT with significant change occurring only in adolescence P45 ($p=0.01$; naïve=50.1±6.9 ng/ml, N=9; ELS=106.1±17.2 ng/ml, N=11, mean±s.e.m.), long after the termination of the stress paradigm (**Fig. 4b**).

Next, we investigated whether increased blood CORT resulted in changes in glucocorticoid receptors (GR) in astrocytes. Using immunostaining with an anti-GR antibody, we found that lateral amygdala astrocytes express this hormone receptor (**Fig. 4c**). Investigation of subcellular localisation of GR within astrocytes, indicative of GR activation and translocation to the nucleus as occurs during canonical GR signalling[53], revealed a clear increase in the intensity of GR expression in the nucleus compared to the cytosol within individual astrocytes ($p=0.026$; naïve=0.23±0.06 a.u., N=8; ELS=0.48±0.08 a.u., N=8; mean±s.e.m.; **Fig. 4d**).

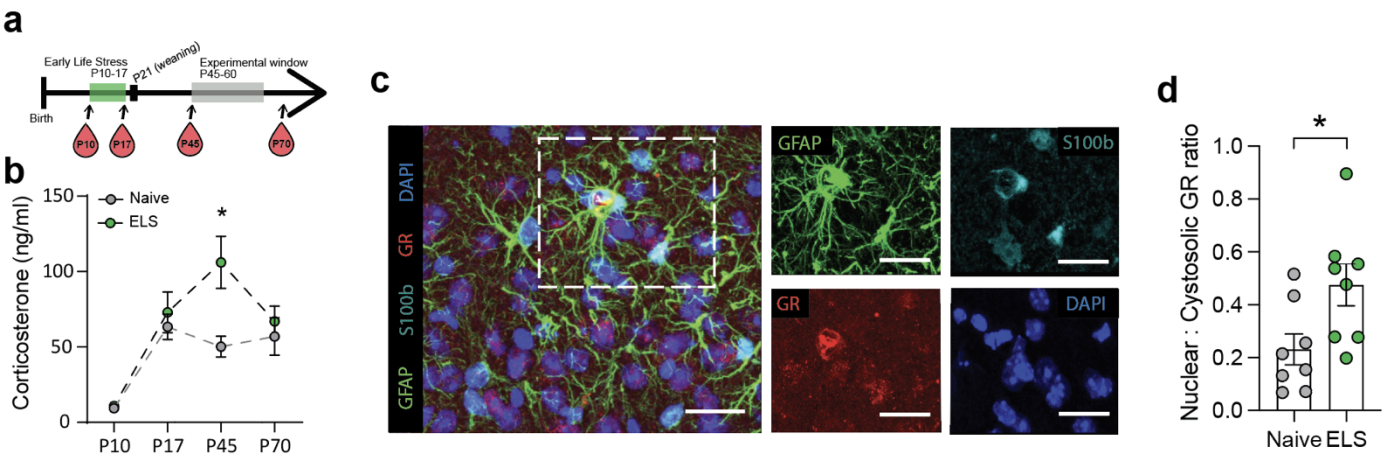

Figure 4. ELS increases blood glucocorticoid levels and translocation of GRs to the nucleus of astrocytes.
(a) Timeline depicting times at which mice were sacrificed and blood was taken for CORT assay. **(b)** Serum corticosterone is significantly increased during adolescence (P45) only, in ELS compared to naïve mice. **(c)** Representative confocal image showing GR immunostaining in astrocytes. Scale bars=20µm. **(d)** Relative expression of GR in the nucleus compared to cytosol was increased in ELS mice.

5. Targeting GR signalling in astrocytes rescues the effects of stress

Thus far, our data suggests that astrocytes respond to early-life stress, resulting in astrocyte dysfunction, subsequent synaptic dysfunction, and cognitive impairment. To test the hypothesis that astrocytic GR signalling mediates the effects of early-life stress on cognitive function we generated a brain region-specific astrocyte GR knockout mouse, injecting an adeno-associated virus to express cre recombinase under the GFAP promoter bilaterally in the lateral amygdala of *nr3c1*-flox mice (**Fig. 5a**). We first validated for specificity and found that it infected predominantly astrocytes using the pan-astrocyte marker S100B (**Suppl. Fig. 3a**) and verified that this did indeed reduce the expression of GR in astrocytes expressing the reporter gene (eGFP) compared to neighbouring astrocytes that did not express the eGFP reporter (**Fig. 5b**). As expected, astrocytes expressing the eGFP reporter showed decreased expression of GR at 53% that of neighbouring non-eGFP expressing astrocytes ($p<0.001$; **Fig. 5c**).

Using this approach, we then determined whether reducing expression of GR specifically in lateral amygdala astrocytes could reverse stress-induced cognitive impairments. Viral injections were carried out following ELS paradigm, between postnatal days P25-35, prior to

behavioural and electrophysiological experiments (**Fig. 5d**). In ELS mice with reduced astrocytic GR expression, we found that learning of auditory discriminative fear conditioning paradigm was improved with a higher freezing to CS+/US pairing ($F_{(1,210)}$=33.3, p<0.001; ELS=41.67±6.9%, N=17; ELS+astroGR KO=55.37±3.5%, N=20, mean±s.e.m.) and lower freezing to CS- ($F_{(1,210)}$=50.1, p<0,001; ELS=13.55±3.5%, N=17; ELS+astroGR KO=2.7±0.7%, N=20; mean±s.e.m.) compared to ELS alone (**Fig. 5h**). This improvement persisted with dramatic improvement in cognitive function with reduced expression of GR in astrocytes. This was evidenced by higher freezing to CS+ ($F_{(1,210)}$=36.96; p<0.001; ELS=58.34±2.3%, N=17; ELS+astroGR KO=73.66±4.3%, N=20) and lower freezing to CS- ($F_{(1,210)}$=215.7, p<0.001; ELS=46.03±2.9%, N=17; ELS+astroGR KO=10.2±1.3%, N=20; **Fig. 5f**), which can be clearly described using the discrimination index ($F_{(1,210)}$=827.6, p<0.001; Group means of DI - ELS=0.12±0.03, N=17. ELS+astroGR KO=0.76±0.03, N=20; mean±s.e.m.; **Fig. 5g**). This genetic manipulation was equally efficient in female and male mice (**Suppl. Fig. 3b**). These data reveal the importance of astrocyte function for amygdala-dependent discrimination of aversive and neutral cues, removing stress signalling in these glial cells dramatically improved performance in this task.

Electrophysiological experiments in brain slices from ELS mice with reduced GR expression in astrocytes showed a trend towards a rescue in plasticity (p=0.08 - ELS vs. ELS astroGR^{KO}; Naïve=164.5±27%, n=12; ELS=106±6.1%, n=13; ELS astroGR^{KO}=140±18.8%, n=12; mean±s.e.m; **Fig. 5h,i**). Together these data highlight the important role of astrocyte glucocorticoid signalling in mediating the long-term effects of ELS on amygdala-dependent behaviour and cognitive function. Importantly, this therapeutic-like intervention, *i.e.* after the stress occurred, was sufficient to reverse the effects of ELS indicating that these important changes remain labile.

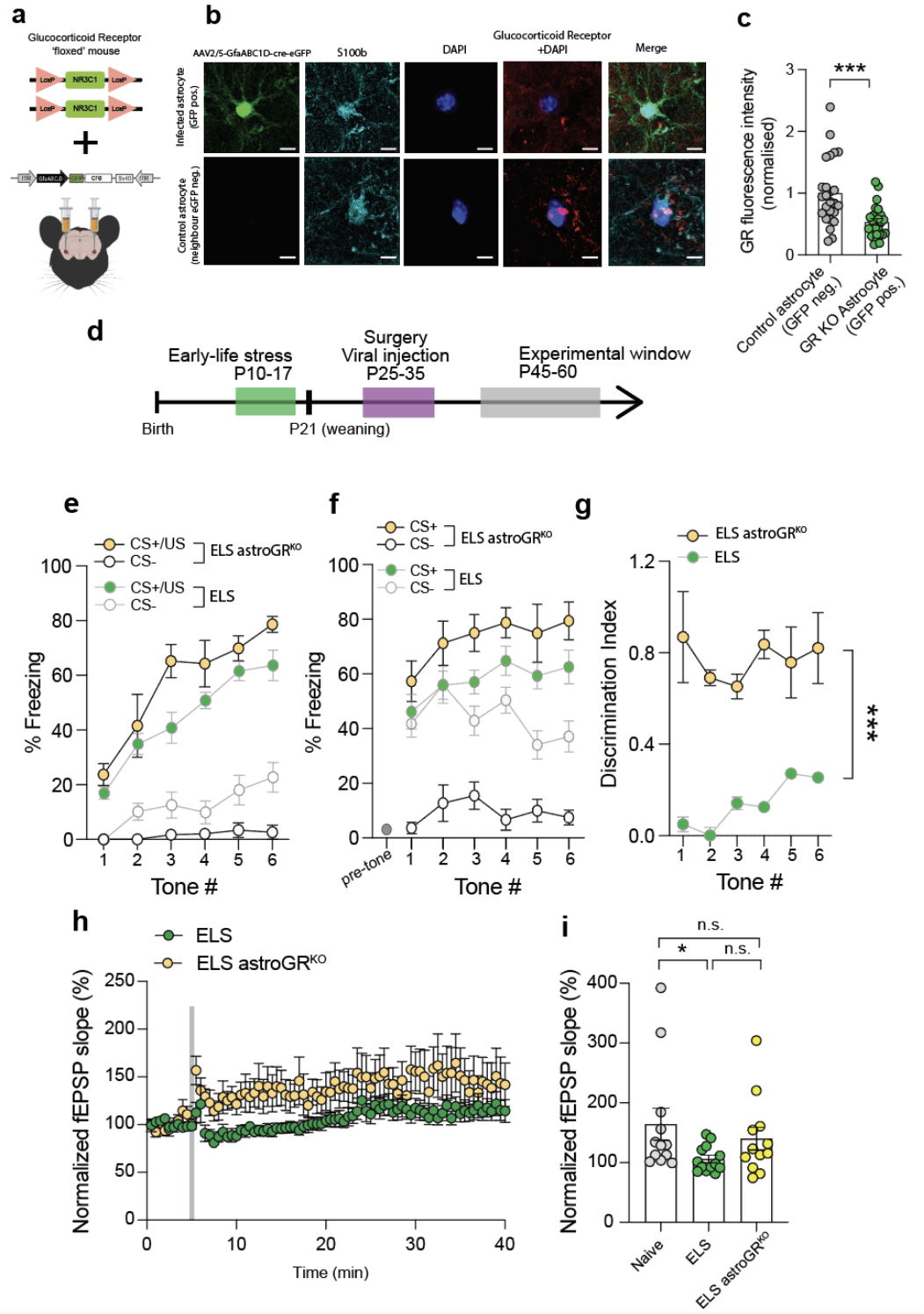

Figure 5. Targeting astrocyte GRs rescues effects of ELS. **(a)** Schematic of lateral amygdala-specific deletion of GR in astrocytes. **(b)** *top row* - Immunostaining of viral infected astrocyte expressing cre-recombinase (and eGFP reporter), S100B confirmation of cell identity, DAPI, GR, and merge of channels. *Bottom row* shows within-brain nearby non-infected astrocyte, lacking eGFP reporter. Scale bars=10µm. **(c)** Quantification of nuclear-GR fluorescence intensity in eGFP negative (control) and eGFP positive (GR KO) astrocytes. **(d)** Timeline highlighting viral injection post-stress, i.e. rescue experiment. **(e)** Comparison of freezing to CS+/US and CS- in ELS (green, grey) and ELS with GR KO in astrocytes (yellow, black). **(f)** Comparison of discrimination between CS+ and CS- during memory recall phase in ELS and ELS with astrocyte GR KO mice. **(g)** Discrimination index is greatly improved with astrocyte GR deletion. **(h)** Normalised field EPSP slope showing synaptic response to theta burst stimulation in ELS and ELS with astrocyte GR KO. **(i)** Bar chart showing normalised fEPSP slope at 30-40min post theta burst stimulation in naïve, ELS, and ELS with astrocyte GR KO.

Discussion:

In this study, we investigated the role of astrocytes in the effects of early-life stress on cognitive function. Using a lateral amygdala-dependent auditory discrimination task, we found that ELS impaired differentiation of neutral from aversive auditory cues and that this cognitive impairment could be completely reversed by reducing glucocorticoid signalling specifically in astrocytes. More precisely, we observed a stress-induced enhancement of freezing to neutral cues, indicative of fear generalisation. This behavioural phenotype was absent in ELS mice in which GR was deleted from astrocytes in the lateral amygdala suggesting that astrocyte function is critical for conferring valence of emotional memory. Furthermore, these data suggest that the hormonal effects of stress on lateral amygdala function are predominantly mediated via astrocyte signalling pathways. This behavioural stress paradigm induced synaptic dysfunction, evidenced by decreased synaptic plasticity in the lateral amygdala, that was partially rescued by astrocyte GR ablation.

In support of the hypothesis that astrocyte dysfunction is responsible for stress-induced cognitive impairment, genetic manipulation of lateral amygdala astrocyte function alone was able to replicate the effects of stress, as evidenced by fear generalisation and synaptic plasticity deficits. These data highlight the importance of astrocytes in mediating the behavioural and synaptic responses to stress. Furthermore, these data reveal that astrocytes are critical for the appropriate behavioural responses to emotionally salient cues, and provide evidence supporting the recently proposed contextual guidance theory of astrocyte function in the brain[30]. Astrocytes have long been shown to be critical for memory formation, with the vast majority of studies reporting that astrocyte dysfunction impairs memory across various brain regions[24,26,32,54]. Here we show that astrocyte dysfunction in the lateral amygdala enhances fear expression evidenced by fear generalisation, *i.e.* the expression of fear towards stimuli of neutral valence. One interpretation of these data is that astrocytes are essential for accurate engram formation[55], with astrocyte dysfunction potentially resulting in a loss of specificity of the memory trace leading to generalisation of fear[46]. Our data are in line with previous reports that have demonstrated clear roles for astrocytes in memory formation and consolidation[24,26,27,32,56,57], and reveal that astrocytes play a key role in stress-induced modifications of emotional memory.

Various distinct ELS paradigms have been shown to influence HPA axis function and circulating stress hormone levels[1,58,59]. Using an ELS paradigm that coincides with peak astrocyte post-natal development[43], we found a latent increase in circulating glucocorticoids after ELS, appearing during adolescence and subsiding towards adulthood. This transient effect may contribute to the enhanced susceptibility to stress observed during adolescence. Similar data has been reported in humans, with levels of circulating cortisol influencing affective disorders[60]. Furthermore, we report increased translocation of GR from the cytosol to the nucleus of astrocytes following ELS, indicative of a higher levels of glucocorticoid signaling[53]. This was associated with changes in expression of key astrocyte proteins including GFAP and Cx43, without a change in GLT-1 suggesting that there is some specificity in the astrocyte response to stress hormones and that efficient clearance of neurotransmitters is a critical function that may be conserved. Although, this static measure of GLT-1 expression levels do not give insight on transporter location and turnover, both of which are critical for efficient synaptic clearance of glutamate[61,62], and could be affected by stress.

To our knowledge, the precise role of astrocyte GRs in the behavioural response to stress remains untested. Considering the strong elevation blood CORT following ELS at a timepoint where we observe cognitive impairments, we tested the hypothesis that astrocyte GR signalling contributed to this phenomenon. Lateral amygdala-specific reduction of astrocyte GR expression revealed the central role played by astrocytes in mediating the effects of stress hormones on this brain circuit. Indeed, reducing GR expression in astrocytes completely reversed cognitive impairment, an observation that strongly supports the growing literature suggesting astrocytes as therapeutic targets for affective disorders[63–65]. The astrocytic impairments induced by ELS, in addition to specific astrocyte disruption (CalEx and dnCx43) that replicate the effect of stress, support the notion that astrocytic modifications are not simply downstream of neuronal dysfunction but rather place astrocytes as key mediators of synaptic and cognitive impairments. Evidence supporting this idea is building across distinct sub-fields. One such example, in a mouse model of Alzheimer's disease, reveals that astrocyte Ca^{2+} hyperactivity precedes and induces synaptic impairments in nearby neurons[66,67]. These ideas are forcing a change in perception of how brain disorders develop and progress moving away from a neuro-centric cascade, placing glial cells in the spotlight[68–73].

In sum, our data place astrocytes as central mediators of the effects of stress on amygdala-dependent behaviour and synaptic function. We also reveal the importance of astrocytes for affective memory with dysfunction of astrocytes in the amygdala resulting in fear generalisation. Taken together, these data support the hypothesis that astrocytes are key to cognitive processing and that dysfunction of astrocytes *via* stress impairs the capacity to execute the appropriate behavioural response to salient cues.

Acknowledgements:

We thank Rosemary Bagot (McGill University) for critical input at the beginning of this study, Thomas Papouin (Washington University in St Louis) for his gift of GR flox mice, Thierry Alquier and Stephanie Fulton (Université de Montréal) for their input throughout. We acknowledge Aurélie Cleret-Buhot (CRCHUM cellular imaging core) for microscopy training and the staff of the animal facility at the CRCHUM. This work was funded by Canadian Institutes of Health Research Project Grant, NSERC Discovery Grant, Fonds de Recherche du Québec – Santé (FRQS), Brain and Behaviour Research Foundation Young Investigator award (NARSAD), CHUM Foundation, and the Réseau Québécois sur le Suicide les troubles de l'humeur et les troubles Associées (RQSHA) grant to C.M-R. I.I.A. and B.R. were both supported by a Canada Graduate Scholarship Master's awards, and Recruitment Fellowships from Neuroscience Dept. Université de Montréal. C.M-R. was supported by a Junior 1 Chercheur-Boursier salary award from FRQS.

Author Contributions:

I.I.A., L.R.D-H, and C.M-R designed the study. I.I.A., J.L-A, J.V. and C.M-R. carried out behavioural experiments, analysing the subsequent data. L.R.D-H. performed viral validation, immunostaining, analysing subsequent data. L.R.D-H, M.D., B.R. took blood samples and performed ELISA experiments. A.B. carried out injection of viral vectors for all experiments, electrophysiological experiments and analysis of subsequent data. S.P. maintained and generated mouse colonies. L.R.D-H, A.B., and C.M-R wrote the manuscript. All authors contributed to ELS paradigm and approved the final version of the manuscript.

Methods:

Animals

All experiments were performed in accordance with the guidelines for maintenance and care of animals of the Canadian Council on Animal Care (CCAC) and approved by the Institutional Committee for the Protection of Animals (CIPA) at the Centre Hospitalier de l'Université de Montréal. Both male and female were used in the study (P45 and P60), housed on a 12hr:12hr light:dark cycle (lights on at 06:30) with *ad libitum* access to food and water.

Generation of Early Life Stress litters

C57bl6j or Nr3c1$^{flx/flx}$ pups were separated from their mothers for 4-hours per day (ZT2-ZT6) for 7 days between ages P10 and P17. During separation pups and mothers were placed into new cages with 60% less bedding. Bedding was weighed on P10 and divided 33% into each cage (home cage, pup separation cage, and mother separation cage). Separated pups and mothers had *ad libitum* access to food and water and pup cages were placed on a water heating pad maintained at 34 degrees Celsius. After the final day of separation (P17) bedding was returned to the original amount and pups were housed with their mothers until weaning at P21.

Behaviour.

Auditory Discriminative Fear Conditioning

Four days prior to behavioural testing mice were single housed in individual cages. Two days later mice were handled for approximately 10 minutes by hand and mobilisation tube. On the first day of ADFC, single housed mice were left for 1 hour in behavioural room to habituate prior to the start of the conditioning assay.

Conditioning: Mice were first exposed to a neutral stimulus (CS-; white noise, 20s) repeated six times. After a two-minute interval mice were exposed to a tone which becomes the conditioned stimulus (CS+;12 kHz tone, 20s) as it co-terminates with a mild foot shock (Unconditioned stimulus (US); 0.5mA, 2s) delivered in the last two seconds of tone presentation (repeated six times; **Fig. 1b,c**). Conditioning was carried out in chamber with checkered walls that was cleaned with 70% ethanol between animals.

Memory recall: 24 hours after conditioning mice were exposed to CS- and CS+ (counterbalanced) in a novel environment characterised by stripped walls and a white floor covering, cleaned with 0.5% hydroperoxide between animals. Fear learning was quantified by the percentage of time spent freezing to CS- and CS+/US during the conditioning phase. Fear memory was quantified by the percentage time freezing to CS- or CS+ following presentation in the memory-recall phase. A discrimination index was calculated comparing fear responses to CS+ and CS- using the following formula;

$$Discrimination\ Index\ (DI) = \frac{(CS^{+}Freezing) - (CS^{-}Freezing)}{(CS^{-}\ Freezing) + (CS^{-}Freezing)}$$

Open Field Task

This task comprised of a total of 5 minutes and during that time the mice were left to freely explore the OFT apparatus, a white plexiglass box measuring 38x38 cm. During the task, mice were filmed, and the time spent in distinct parts of the box *i.e.* centre and periphery were quantified using AnyMaze software (Stoelting). The total time spent in the center was used as a quantification of anxiety-like behaviour, where more time in the center represented anti-anxious behaviour and the total distance travelled was measured to quantify locomotor impairments.

Elevated Plus Maze

This task comprised of a total of 5 minutes during which mice were removed from their cages and placed at the centre of the four arms of the maze, facing an open arm. Mice were video recorded, and these videos were analysed using Anymaze software (Stoelting) which quantified the number of entries and the time spent (s) in closed arms or open arms during the 5min testing period. Anxiety-like behaviour was quantified by both the number of entries into, and the duration spent in the open arms.

Slice preparation

Coronal slices containing lateral amygdala were obtained from mice between P45-60. Animals were anesthetized with isoflurane and the brain was rapidly excised and placed in ice-cold

choline-based cutting solution saturated with 95% O_2 and 5% CO_2 containing the following (in mM): 120 choline chloride, 3 KCl, 1.25 NaH_2PO_4, 26 $NaHCO_3$, 8 $MgCl_2$, 20 glucose, pH 7.2 and 295 mOsmol. Slices (300 µm thick) were cut on a vibratome (Leica VT1200, Nussloch, Germany). Slices were transferred to oxygenated artificial CSF (ACSF) at 32 ± 0.5°C for 30 min containing the following (in mM): 130 NaCl, 2.5 KCl, 1.25 NaH_2PO_4, 26 $NaHCO_3$, 10 glucose, 1.3 $MgCl_2$, 2 $CaCl_2$, pH 7.3–7.4 and 300-305 mOsmol, then allowed to recover for at least 30 min before recordings in oxygenated ACSF at room temperature (RT). For experiments, the slices were transferred to a recording chamber where they were perfused (2 ml/min) with ACSF at 32ºC for the course of the experiment. Slices were used for a maximum of 6 hr after cutting.

Electrophysiology

Extracellular field excitatory postsynaptic potentials (fEPSPs) were recorded in current clamp mode with a pipette filled with ACSF placed in the lateral part of the amygdala. Monosynaptic EPSCs were elicited by stimulation of cortical afferences with a tungsten concentric bipolar electrode (World Precision Instruments). The theta burst stimulation (TBS) lasted 10s consisting of 4 pulses at 100 Hz repeated at 5 Hz intervals. Signals were amplified using a Multiclamp 700B amplifier (Molecular Devices) and digitized using the Digidata 1440 (Molecular Devices). Data were recorded (pClamp 10.2, Molecular Devices) for offline analysis. The magnitude of LTP was quantified by normalizing and averaging the slope of fEPSPs following LTP induction relative to the last 5 min of baseline.

Stereotaxic surgery and AAV delivery

P25-35 mice were given a subcutaneous (*sc,*) injection of Carprofen (20 mg/kg) 1h prior surgery. Animals were then deeply anesthetised (2% isoflurane) before placing them into a stereotaxic frame (Kopf instruments). Surgical site was infiltrated with bupivacaine/lidocaine (2mg/kg *sc.*) 15 min prior surgery. Biliteral injections of the following viral constructs: AAV2/5-gfaABC1D-CRE-2A-eGFP (1.2-1.7x10^^{12} GC/ml); AAV2/5-gfaABC1D-eGFP (1.2-1.5x10^$^{11-12}$ GC/ml) and AAV2/5-gfaABC1D-hPMCAw/b-mCherry (1.2x10^^{12}) were delivered to the LA (coordinates relative to bregma: -1.4 mm AP, ± 3.4 mm ML and -5 mm DV) of mice of either sex. Viral solutions were injected at a rate of 200 nL/min for a total volume of 650 nL per hemisphere using a 10 µl

Hamilton syringe (Harvard apparatus) and a microinjection syringe pump (UMP3T-2 World Precision Instruments). Animals received 250 µL of saline for post-surgery hydration.

Brain processing.

Mice were anaesthetised in an enclosed chamber filled with isoflurane (5% for induction, 3-4% for maintenance, v/v) until loss of toe pinch reflex. A transcardial perfusion was used to ensure uniform preservation of tissue and brains were fixed in 4 % paraformaldehyde (PFA) for 24 hours at 4 degrees Celsius. The fixed brains were then placed in falcon tubes containing 30% sucrose solution for a minimum of two days. Brains were embedded in optimal cutting temperature (OCT) compound and flash frozen in 2-methylbutane between -40 and -50 degrees Celsius and then stored at -80 until cryosectioning. Brains were cut a 30um thickness at -20 degrees Celsius using a Leica CM3050S Cryostat. Slices were stored in cryoprotector solution at 4 degrees Celsius until immunohistochemistry.

Immunohistochemistry.

Free floating brain slices were washed 3 times in 1X PBS for 15 minutes to remove cryoprotector solution. Slices were permeabilised in block-perm solution (3% Bovine-Serum-Albumin, 0.5% Triton$^{10\%}$ in PBS) for a duration of 1 hour. Slices were incubated with antibodies for 24 hours at 4 degrees Celsius. Slices were incubated with primary antibodies; [Rabbit] anti-S100ß (1:1000, Abcam, ab52642), [Mouse] anti-glucocorticoid receptor (1:500, ThermoFisher, MA1-510), [Chicken] anti-GFAP (1:1000, ThermoFisher, PA1-10004), [mouse] anti-Cx43 (1:1000 ThermoFisher, 3D8A5) and [Rabbit Anti-GLT-1 (EAAT2) (1:1000, NovusBio, NBP1-20136). After primary antibody incubation slices were washed 3 times in 1X PBS for 15 minutes to remove non-specific binding. Slices were incubated with secondary antibodies in a DAPI solution (1:10000) at RT in aluminium foil for 1 hour. Slices were incubated with secondary antibodies; [goat] anti-rabbit Alexa 488 (1:1000, Jackson Immuno Research, 111-545-144), [goat] anti-mouse Alexa 647 (1:1000, ThermoFisher, A32728), [goat] anti-chicken Alexa 568 (1:1000, ThermoFisher, A11041). After secondary antibody incubation slices were washed again 3 times in 1X PBS for 15 minutes before being mounted onto Fisherbrand microscope slides using ProLong™ Glass Antifade mountant (P36982).

Microscopy

Slices were imaged using a Leica TCS SP5 laser scanning confocal microscope with oil immersion Plan-Apochromat 63x objective 1.4 NA. 16-bit images of 246 x 246 um areas were acquired at 400Hz (frame size (x*y); 1024 x 1024, pixel size; 250nm). 25-30um z-stacks were acquired with a step size of 0.5um. 15um max intensity z-projections of the lateral amygdala were analysed using Image-J (Fiji) to obtain A.U fluorescence intensity measures of secondary antibodies attached to primaries with specificity to epitopes; GFAP, Cx43, GLT-1, and Glucocorticoid-Receptor. We applied a fluorescence threshold for GFAP, Cx43 and GLT-1 fluorescence and measured integrated density A.U (thresholds; Mean, Otsu, Otsu respectively). For nuclear and cytosolic Glucocorticoid Receptor measures, astrocyte (s100b+) DAPI nuclei were thresholded and used as ROIs for nuclear measures of GR fluorescence ($S100b^+$ + $DAPI^+$). The same nuclear DAPI ROI was cleared from the previously thresholded s100b regions to obtain cytosolic astrocytic GR ($S100b^+$ - $DAPI^+$). Integrated density A.U of GR fluorescence was used to calculate Nuclear:Cytosolic GR ratios.

Blood Collection & Corticosterone analysis

Trunk blood was collected via decapitation at ZT2 (08:30). To minimise handling induced elevations in corticosterone mice were housed with clear plastic tubes used to move individual mice intoan enclosed chamber filled with isoflurane 5% for 2 minutes. Mice were placed in enclosed Isoflurane until loss of toe pinch reflect (maximum elapsed time of 2 minutes). Mice were decapitated and trunk blood was collected into BD 365963 Microtainer® Capillary Blood Collection Tubes and placed onto Ice. Blood was centrifuged for 5 minutes at 4 degrees Celsius at 5000rpm. Serum was aliquoted and stored at -80 degrees Celsius. Corticosterone measurements were obtained using an ENZO ELISA kit (ADI-900-097).

Statistical analyses

Results are presented as mean ±SEM. Data with one variable were analyzed with the two-tailed Student's *t* test or Mann-Whitney test. Data with more than two conditions were first screened for a Gaussian distribution with Kolmogorov-Smirnov test followed by analysis either with one-way/repeated measures ANOVA or Kruskal-Wallis/Friedman test when needed and Tukey's multiple-comparison parametric *post hoc* test (data with Gaussian distribution) or by a

Dunn`s multiple-comparison non-parametric *post hoc* test (data with non-Gaussian distribution). Auditory discriminative fear conditioning data was analysed using a two-way ANOVA with appropriate post-hoc tests. Open field and elevated plus maze data analysed using one-way ANOVA with appropriate post hoc tests. Graphic significance levels were *, $p < 0.05$; **, $p < 0.01$ and ***, $p < 0.001$. All data were analyzed using GraphPad Prism software (Version 9, GraphPad, USA).

Data availability

The datasets that support the findings of this study are available from the corresponding author upon reasonable request

References :

1. Walker, C.-D. *et al.* Chronic early life stress induced by limited bedding and nesting (LBN) material in rodents: critical considerations of methodology, outcomes and translational potential. *Stress Amst. Neth.* **20**, 421–448 (2017).
2. Joëls, M. & Baram, T. Z. The neuro-symphony of stress. *Nat. Rev. Neurosci.* **10**, 459–466 (2009).
3. Lopez, J. & Bagot, R. C. Defining Valid Chronic Stress Models for Depression With Female Rodents. *Biol. Psychiatry* **90**, 226–235 (2021).
4. O'Donnell, K. J. & Meaney, M. J. Epigenetics, Development, and Psychopathology. *Annu. Rev. Clin. Psychol.* **16**, 327–350 (2020).
5. Meaney, M. J. Maternal Care, Gene Expression, and the Transmission of Individual Differences in Stress Reactivity Across Generations. *Annu. Rev. Neurosci.* **24**, 1161–1192 (2001).
6. Peña, C. J. *et al.* Early life stress confers lifelong stress susceptibility in mice via ventral tegmental area OTX2. *Science* **356**, 1185–1188 (2017).
7. Kosten, T. A., Lee, H. J. & Kim, J. J. Early life stress impairs fear conditioning in adult male and female rats. *Brain Res.* **1087**, 142–150 (2006).
8. Lesuis, S. L., Lucassen, P. J. & Krugers, H. J. Early life stress impairs fear memory and synaptic plasticity; a potential role for GluN2B. *Neuropharmacology* **149**, 195–203 (2019).
9. Peña, C. J., Nestler, E. J. & Bagot, R. C. Environmental Programming of Susceptibility and Resilience to Stress in Adulthood in Male Mice. *Front. Behav. Neurosci.* **13**, 40 (2019).
10. Peña, C. J. *et al.* Early life stress alters transcriptomic patterning across reward circuitry in male and female mice. *Nat. Commun.* **10**, 5098 (2019).

11. Lupien, S. J., McEwen, B. S., Gunnar, M. R. & Heim, C. Effects of stress throughout the lifespan on the brain, behaviour and cognition. *Nat. Rev. Neurosci.* **10**, 434–445 (2009).

12. Ulrich-Lai, Y. M. & Herman, J. P. Neural regulation of endocrine and autonomic stress responses. *Nat. Rev. Neurosci.* **10**, 397–409 (2009).

13. Bains, J. S., Wamsteeker Cusulin, J. I. & Inoue, W. Stress-related synaptic plasticity in the hypothalamus. *Nat. Rev. Neurosci.* **16**, 377–388 (2015).

14. Guadagno, A., Belliveau, C., Mechawar, N. & Walker, C.-D. Effects of Early Life Stress on the Developing Basolateral Amygdala-Prefrontal Cortex Circuit: The Emerging Role of Local Inhibition and Perineuronal Nets. *Front. Hum. Neurosci.* **15**, (2021).

15. Murphy-Royal, C. *et al.* Stress gates an astrocytic energy reservoir to impair synaptic plasticity. *Nat. Commun.* **11**, 2014 (2020).

16. Lau, B. K. *et al.* Obesity-induced astrocyte dysfunction impairs heterosynaptic plasticity in the orbitofrontal cortex. *Cell Rep.* **36**, 109563 (2021).

17. Henneberger, C., Papouin, T., Oliet, S. H. R. & Rusakov, D. A. Long-term potentiation depends on release of D-serine from astrocytes. *Nature* **463**, 232–236 (2010).

18. Covelo, A. & Araque, A. Neuronal activity determines distinct gliotransmitter release from a single astrocyte. *eLife* **7**, e32237 (2018).

19. Panatier, A. *et al.* Astrocytes are endogenous regulators of basal transmission at central synapses. *Cell* **146**, 785–798 (2011).

20. Doron, A. *et al.* Hippocampal astrocytes encode reward location. *Nature* **609**, 772–778 (2022).

21. Mu, Y. *et al.* Glia Accumulate Evidence that Actions Are Futile and Suppress Unsuccessful Behavior. *Cell* **178**, 27-43.e19 (2019).

22. Yu, X. *et al.* Reducing Astrocyte Calcium Signaling In Vivo Alters Striatal Microcircuits and Causes Repetitive Behavior. *Neuron* **99**, 1170-1187.e9 (2018).

23. Jimenez-Blasco, D. *et al.* Glucose metabolism links astroglial mitochondria to cannabinoid effects. *Nature* **583**, 603–608 (2020).

24. Suzuki, A. *et al.* Astrocyte-neuron lactate transport is required for long-term memory formation. *Cell* **144**, 810–823 (2011).

25. Wang, J. *et al.* Astrocytic l-Lactate Signaling Facilitates Amygdala-Anterior Cingulate Cortex Synchrony and Decision Making in Rats. *Cell Rep.* **21**, 2407–2418 (2017).

26. Kol, A. *et al.* Astrocytes contribute to remote memory formation by modulating hippocampal–cortical communication during learning. *Nat. Neurosci.* **23**, 1229–1239 (2020).

27. Adamsky, A. *et al.* Astrocytic Activation Generates De Novo Neuronal Potentiation and Memory Enhancement. *Cell* **174**, 59-71.e14 (2018).

28. Papouin, T., Dunphy, J. M., Tolman, M., Dineley, K. T. & Haydon, P. G. Septal Cholinergic Neuromodulation Tunes the Astrocyte-Dependent Gating of Hippocampal NMDA Receptors to Wakefulness. *Neuron* **94**, 840-854.e7 (2017).

29. Robin, L. M. *et al.* Astroglial CB1 Receptors Determine Synaptic D-Serine Availability to Enable Recognition Memory. *Neuron* **98**, 935-944.e5 (2018).

30. Murphy-Royal, C., Ching, S. & Papouin, T. Contextual guidance: An integrated theory for astrocytes function in brain circuits and behavior. Preprint at https://doi.org/10.48550/arXiv.2211.09906 (2022).

31. Wahis, J. *et al.* Astrocytes mediate the effect of oxytocin in the central amygdala on neuronal activity and affective states in rodents. *Nat. Neurosci.* **24**, 529–541 (2021).

32. Martin-Fernandez, M. *et al.* Synapse-specific astrocyte gating of amygdala-related behavior. *Nat. Neurosci.* **20**, 1540–1548 (2017).

33. Corkrum, M. *et al.* Dopamine-Evoked Synaptic Regulation in the Nucleus Accumbens Requires Astrocyte Activity. *Neuron* **105**, 1036-1047.e5 (2020).

34. Ressler, K. J. Amygdala Activity, Fear, and Anxiety: Modulation by Stress. *Biol. Psychiatry* **67**, 1117–1119 (2010).

35. Roozendaal, B., McEwen, B. S. & Chattarji, S. Stress, memory and the amygdala. *Nat. Rev. Neurosci.* **10**, 423–433 (2009).

36. Johnson, F. K. *et al.* Amygdala hyper-connectivity in a mouse model of unpredictable early life stress. *Transl. Psychiatry* **8**, 49 (2018).

37. Malter Cohen, M. *et al.* Early-life stress has persistent effects on amygdala function and development in mice and humans. *Proc. Natl. Acad. Sci. U. S. A.* **110**, 18274–18278 (2013).

38. Guadagno, A., Wong, T. P. & Walker, C.-D. Morphological and functional changes in the preweaning basolateral amygdala induced by early chronic stress associate with anxiety and fear behavior in adult male, but not female rats. *Prog. Neuropsychopharmacol. Biol. Psychiatry* **81**, 25–37 (2018).

39. Guadagno, A. *et al.* Reduced resting-state functional connectivity of the basolateral amygdala to the medial prefrontal cortex in preweaning rats exposed to chronic early-life stress. *Brain Struct. Funct.* **223**, 3711–3729 (2018).

40. Kim, W. B. & Cho, J.-H. Encoding of Discriminative Fear Memory by Input-Specific LTP in the Amygdala. *Neuron* **95**, 1129-1146.e5 (2017).

41. Rogan, M. T., Stäubli, U. V. & LeDoux, J. E. Fear conditioning induces associative long-term potentiation in the amygdala. *Nature* **390**, 604–607 (1997).

42. Duvarci, S. & Pare, D. Amygdala microcircuits controlling learned fear. *Neuron* **82**, 966–980 (2014).

43. Rurak, G. M. *et al.* Sex differences in developmental patterns of neocortical astroglia: A mouse translatome database. *Cell Rep.* **38**, 110310 (2022).

44. Farhy-Tselnicker, I. & Allen, N. J. Astrocytes, neurons, synapses: a tripartite view on cortical circuit development. *Neural Develop.* **13**, 7 (2018).

45. Han, J.-H. *et al.* Selective erasure of a fear memory. *Science* **323**, 1492–1496 (2009).

46. Rashid, A. J. *et al.* Competition between engrams influences fear memory formation and recall. *Science* **353**, 383–387 (2016).

47. LeDoux, J., Cicchetti, P., Xagoraris, A. & Romanski, L. The lateral amygdaloid nucleus: sensory interface of the amygdala in fear conditioning. *J. Neurosci.* **10**, 1062–1069 (1990).

48. Giaume, C., Koulakoff, A., Roux, L., Holcman, D. & Rouach, N. Astroglial networks: a step further in neuroglial and gliovascular interactions. *Nat. Rev. Neurosci.* **11**, 87–99 (2010).

49. Murphy-Royal, C., Dupuis, J., Groc, L. & Oliet, S. H. R. Astroglial glutamate transporters in the brain: Regulating neurotransmitter homeostasis and synaptic transmission. *J. Neurosci. Res.* **95**, 2140–2151 (2017).

50. Institoris, A. *et al.* Astrocytes amplify neurovascular coupling to sustained activation of neocortex in awake mice. 2020.12.16.422785 Preprint at https://doi.org/10.1101/2020.12.16.422785 (2022).

51. Carter, B., Hamilton, D. & Thompson, R. Acute and chronic glucocorticoid treatments regulate astrocyte-enriched mRNAs in multiple brain regions in vivo. *Front. Neurosci.* **7**, (2013).

52. Allaman, I., Pellerin, L. & Magistretti, P. J. Glucocorticoids modulate neurotransmitter-induced glycogen metabolism in cultured cortical astrocytes. *J. Neurochem.* **88**, 900–908 (2004).

53. de Kloet, E. R., Joëls, M. & Holsboer, F. Stress and the brain: from adaptation to disease. *Nat. Rev. Neurosci.* **6**, 463–475 (2005).

54. Li, Y. *et al.* Activation of astrocytes in hippocampus decreases fear memory through adenosine A1 receptors. *eLife* **9**, e57155 (2020).

55. Josselyn, S. A., Köhler, S. & Frankland, P. W. Finding the engram. *Nat. Rev. Neurosci.* **16**, 521–534 (2015).

56. Gibbs, M. E., Anderson, D. G. & Hertz, L. Inhibition of glycogenolysis in astrocytes interrupts memory consolidation in young chickens. *Glia* **54**, 214–222 (2006).

57. Tertil, M. *et al.* Glucocorticoid receptor signaling in astrocytes is required for aversive memory formation. *Transl. Psychiatry* **8**, 255 (2018).

58. Molet, J., Maras, P. M., Avishai-Eliner, S. & Baram, T. Z. Naturalistic rodent models of chronic early-life stress. *Dev. Psychobiol.* **56**, 1675–1688 (2014).

59. Raineki, C., Moriceau, S. & Sullivan, R. M. Developing a Neurobehavioral Animal Model of Infant Attachment to an Abusive Caregiver. *Biol. Psychiatry* **67**, 1137–1145 (2010).

60. Ellenbogen, M. A., Hodgins, S., Walker, C.-D., Couture, S. & Adam, S. Daytime cortisol and stress reactivity in the offspring of parents with bipolar disorder. *Psychoneuroendocrinology* **31**, 1164–1180 (2006).

61. Murphy-Royal, C. *et al.* Surface diffusion of astrocytic glutamate transporters shapes synaptic transmission. *Nat. Neurosci.* **18**, 219–226 (2015).

62. Al Awabdh, S. *et al.* Neuronal activity mediated regulation of glutamate transporter GLT-1 surface diffusion in rat astrocytes in dissociated and slice cultures. *Glia* **64**, 1252–1264 (2016).

63. Kaul, D., Schwab, S. G., Mechawar, N., Ooi, L. & Matosin, N. Alterations in Astrocytic Regulation of Excitation and Inhibition by Stress Exposure and in Severe Psychopathology. *J. Neurosci.* **42**, 6823–6834 (2022).

64. O'Leary, L. A. & Mechawar, N. Implication of cerebral astrocytes in major depression: a review of fine neuroanatomical evidence in humans. *Glia* **69**, 2077–2099 (2021).

65. Nagy, C. *et al.* Astrocytic abnormalities and global DNA methylation patterns in depression and suicide. *Mol. Psychiatry* **20**, 320–328 (2015).

66. Bosson, A. *et al.* TRPA1 channels promote astrocytic Ca2+ hyperactivity and synaptic dysfunction mediated by oligomeric forms of amyloid-β peptide. *Mol. Neurodegener.* **12**, 53 (2017).

67. Paumier, A. *et al.* Astrocyte-neuron interplay is critical for Alzheimer's disease pathogenesis and is rescued by TRPA1 channel blockade. *Brain J. Neurol.* **145**, 388–405 (2022).

68. Guttenplan, K. A. *et al.* Neurotoxic reactive astrocytes induce cell death via saturated lipids. *Nature* **599**, 102–107 (2021).

69. Williamson, M. R., Fuertes, C. J. A., Dunn, A. K., Drew, M. R. & Jones, T. A. Reactive astrocytes facilitate vascular repair and remodeling after stroke. *Cell Rep.* **35**, 109048 (2021).

70. De Strooper, B. & Karran, E. The Cellular Phase of Alzheimer's Disease. *Cell* **164**, 603–615 (2016).

71. Escartin, C. *et al.* Reactive astrocyte nomenclature, definitions, and future directions. *Nat. Neurosci.* **24**, 312–325 (2021).

72. Brandebura, A. N., Paumier, A., Onur, T. S. & Allen, N. J. Astrocyte contribution to dysfunction, risk and progression in neurodegenerative disorders. *Nat. Rev. Neurosci.* (2022) doi:10.1038/s41583-022-00641-1.

73. Murphy-Royal, C., Gordon, G. R. & Bains, J. S. Stress-induced structural and functional modifications of astrocytes-Further implicating glia in the central response to stress. *Glia* **67**, 1806–1820 (2019).

Figure 1 - Effects of ELS on behaviour and synaptic function

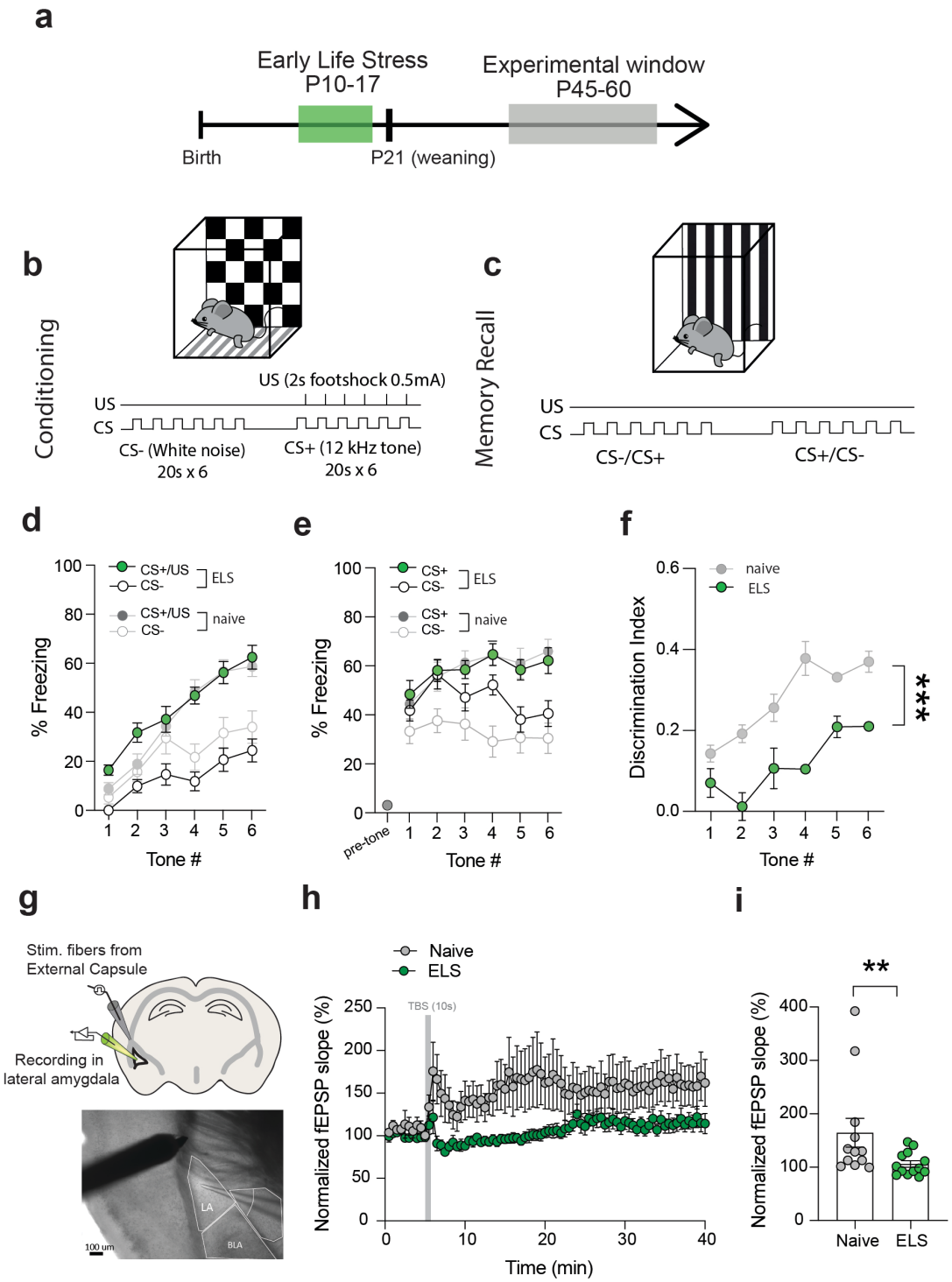

Figure 2 - Impact of ELS on astrocytes

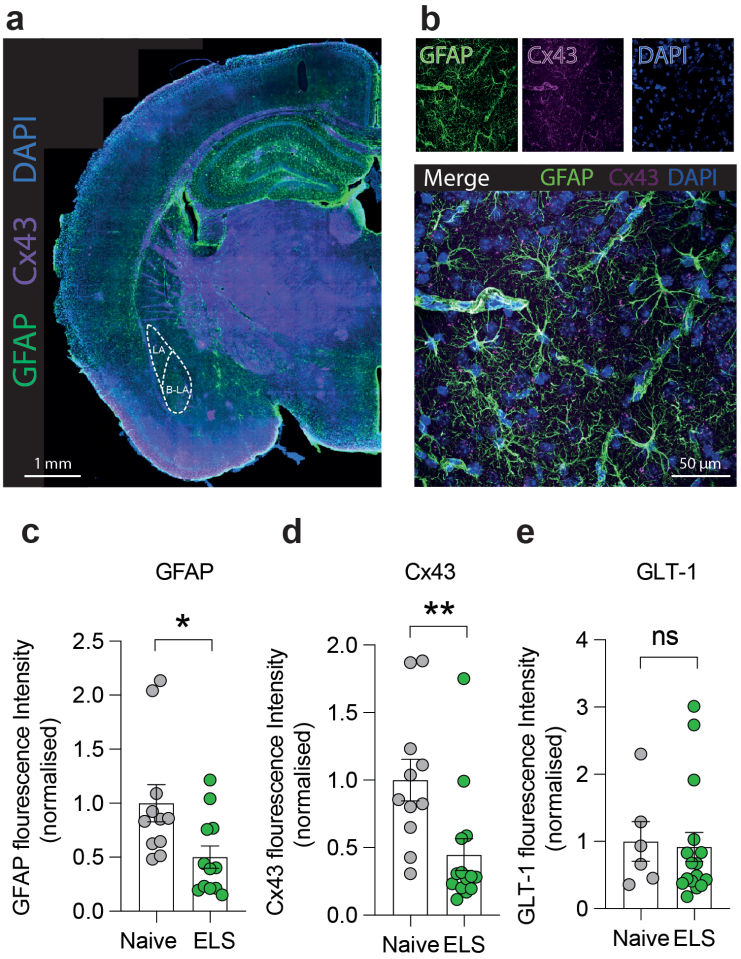

Figure 3 - Astrocyte dysfunction alone mirrors effects of ELS on behaviour and synapses

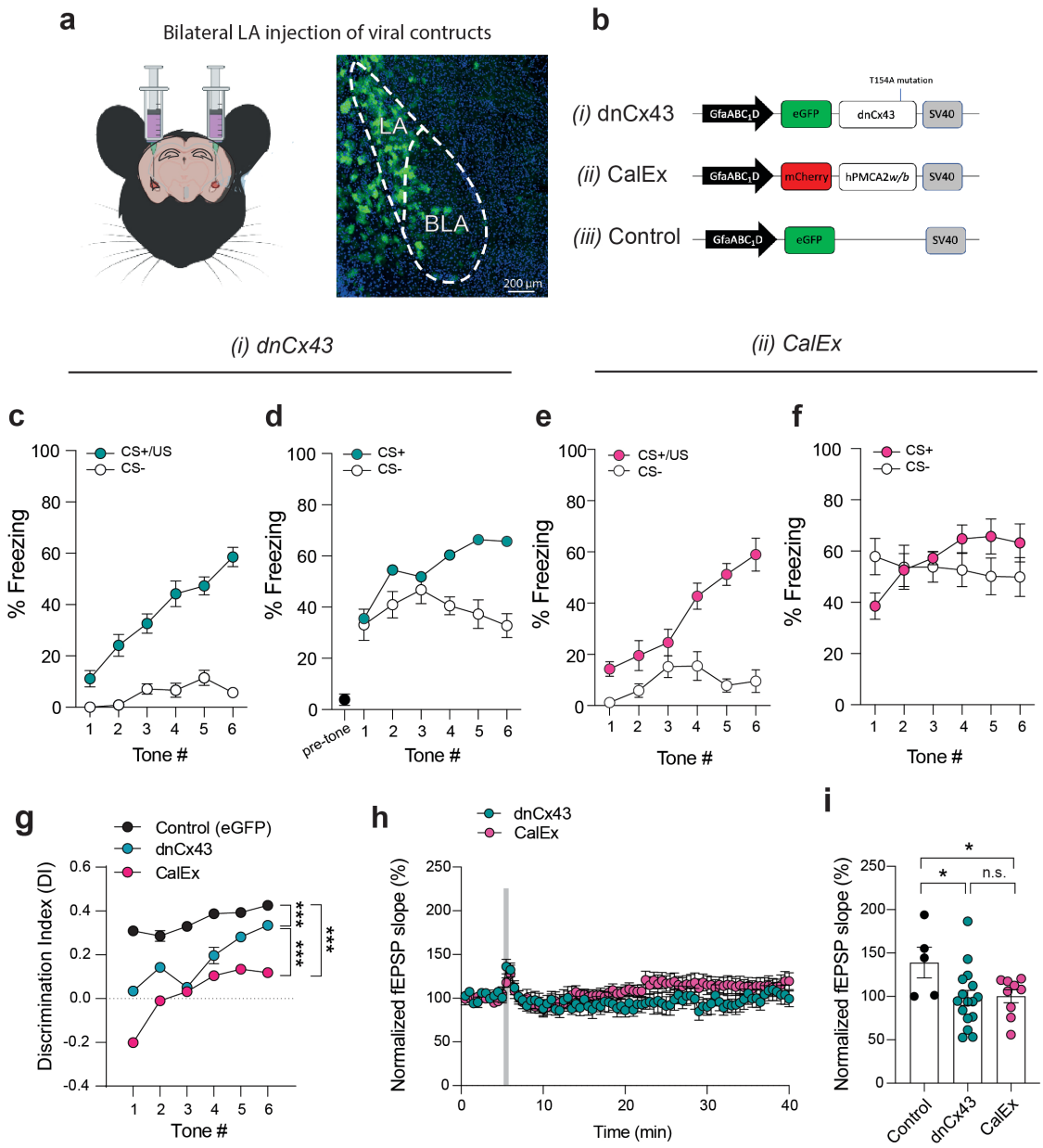

Figure 4 - ELS increases blood glucocorticoid levels and translocation of GRs to the nucleus of astrocytes

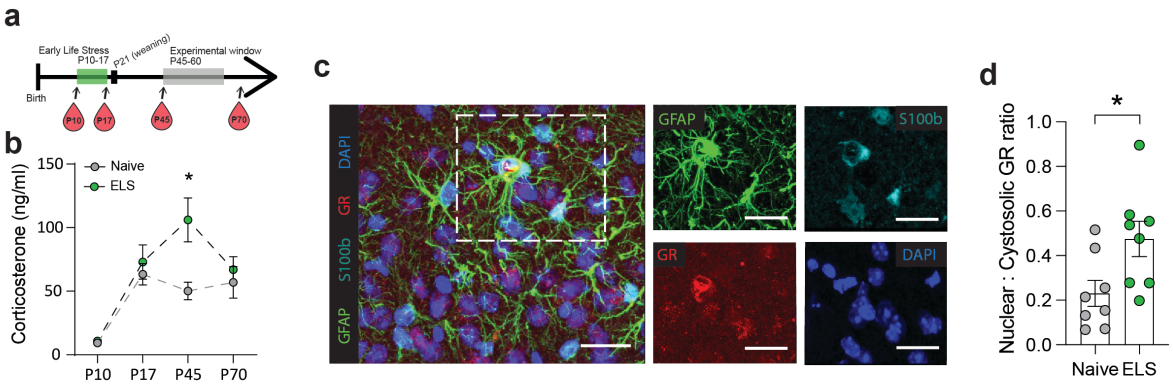

Figure 5 - Targeting astrocyte GRs rescues effects of ELS

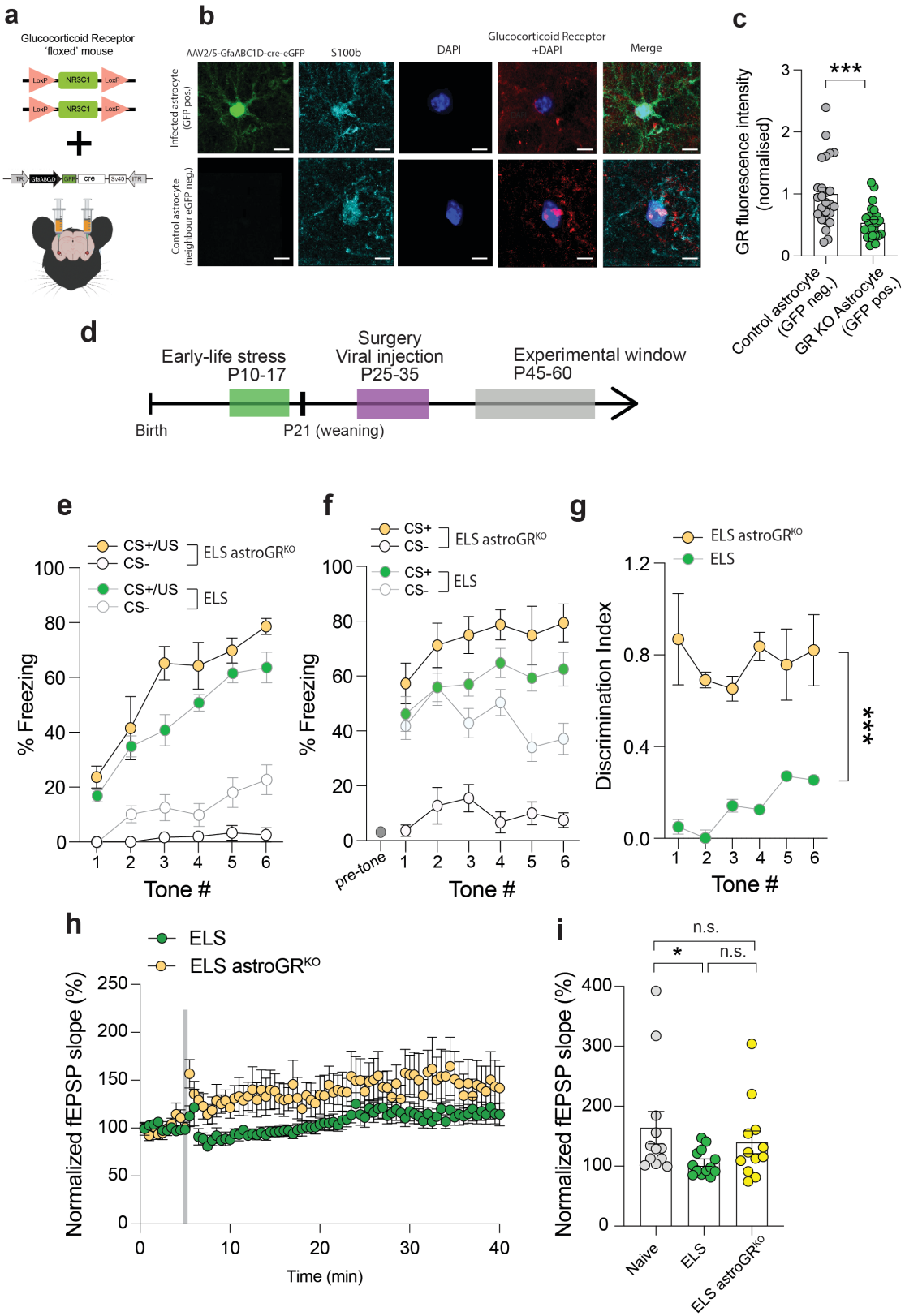

Supplementary Figure 1

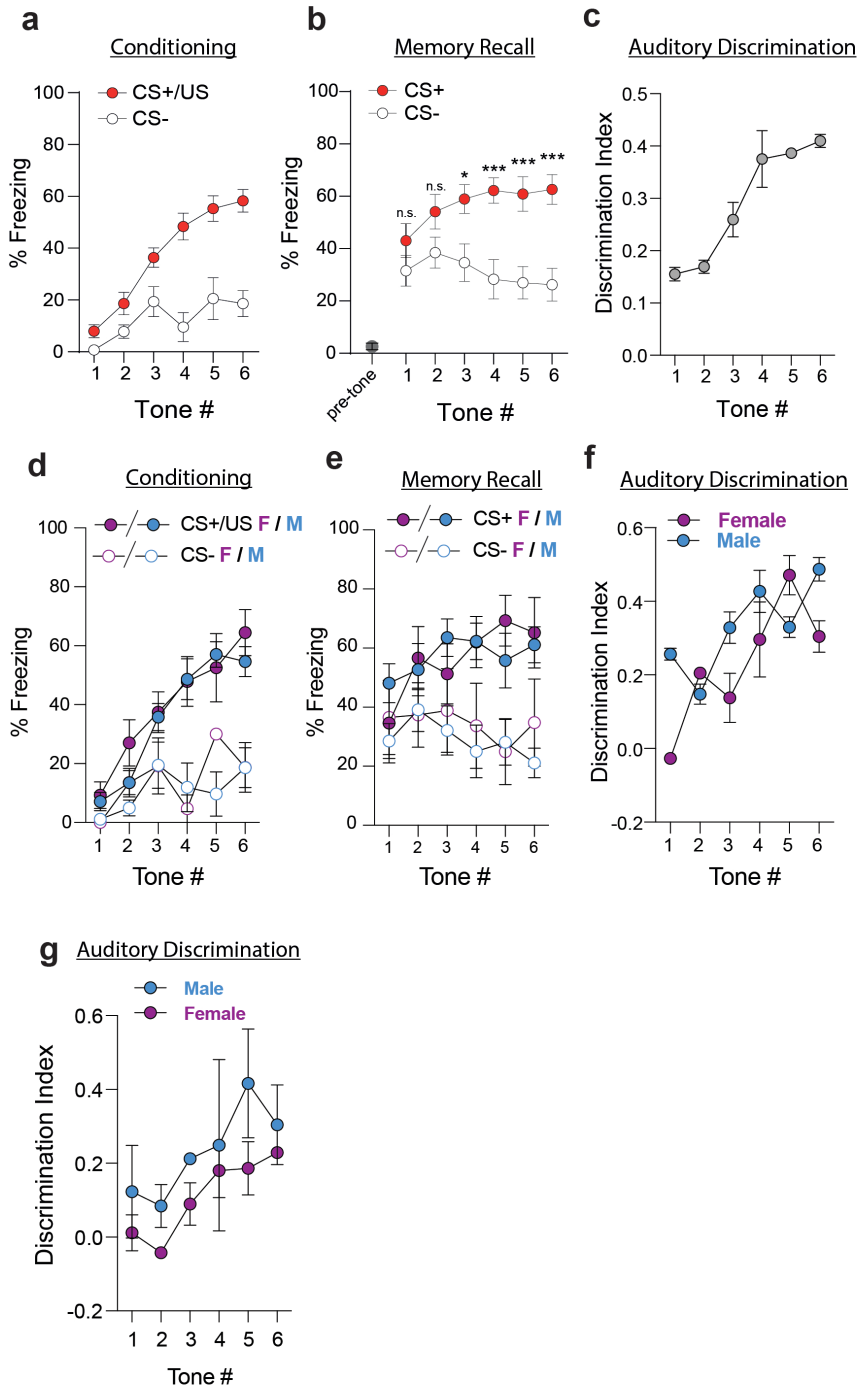

Supplementary Figure 2

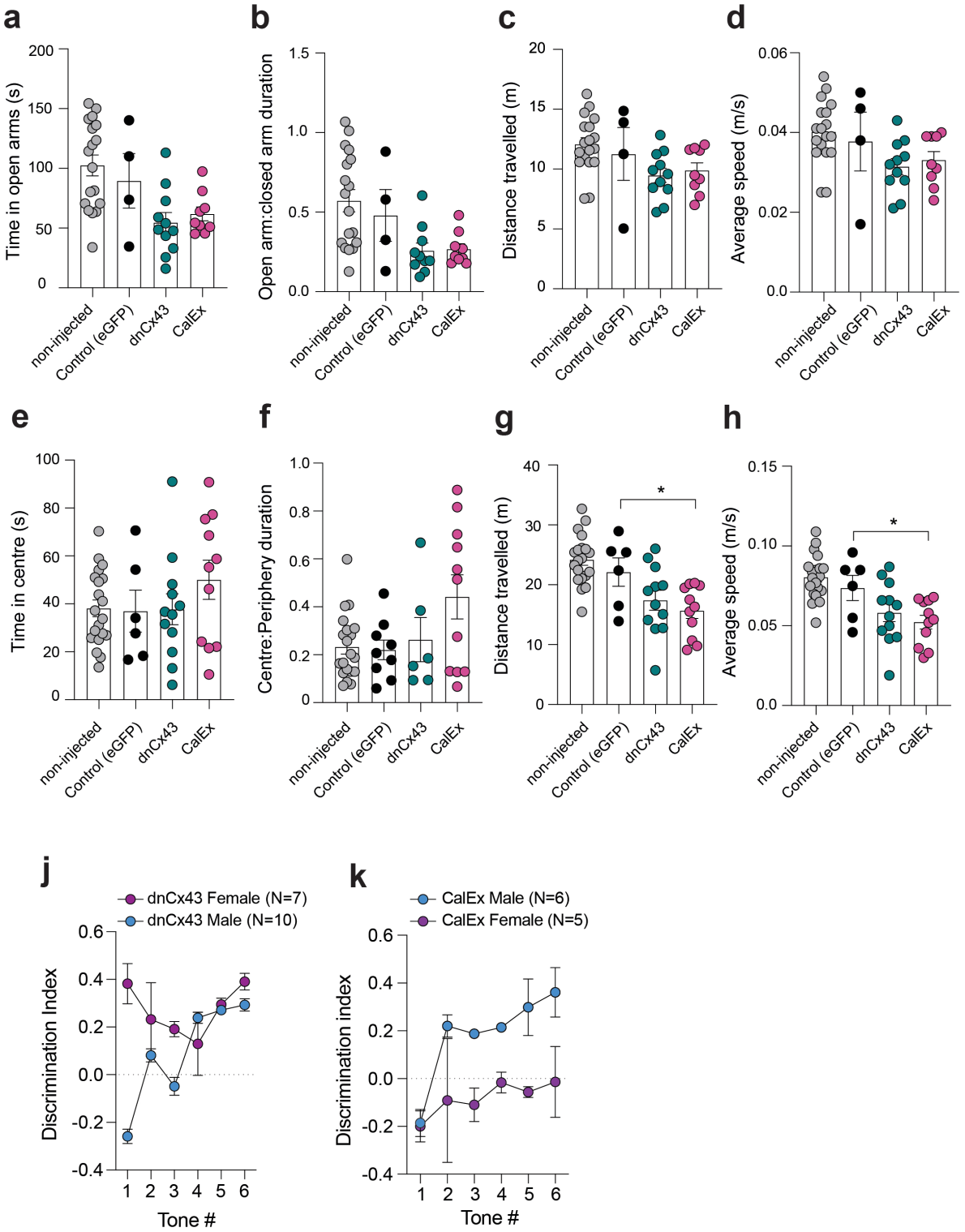

Supplementary Figure 3

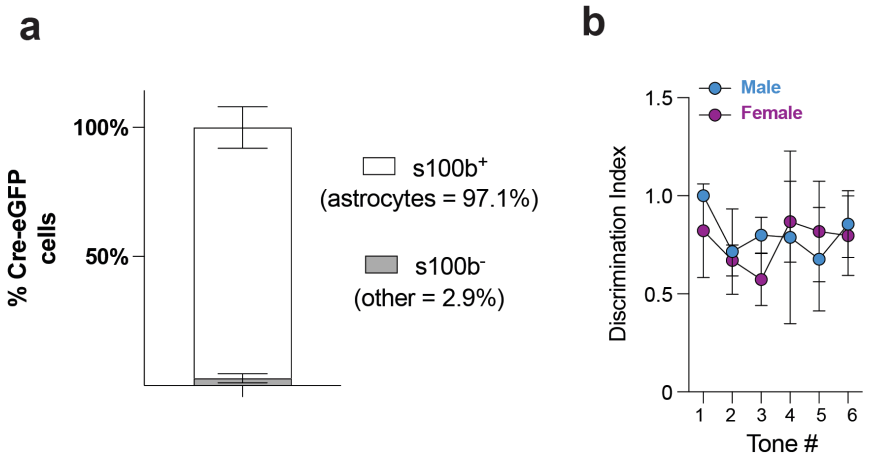

Figure Legends:

Figure 1. Effects of ELS on behaviour and synaptic function.
(a) Timeline of experimental paradigm. **(b)** Schematic representation of conditioning phase of auditory discriminative fear conditioning, and **(c)** memory recall phase. **(d)** Comparison of percentage of time spent freezing during CS+/US and CS- presentation during conditioning in ELS and naïve mice. **(e)** Comparison of percentage of time spent freezing during memory recall phase in ELS and naïve mice. **(f)** Comparison of discrimination between CS+ and CS- during memory recall phase in ELS and naïve mice. **(g)** *top* Schematic representation of electrophysiology stimulation and recording sites. *bottom* DIC image of stimulating and recording electrodes in an acute brain slice. **(h)** Average trace of field EPSP slope showing synaptic response to theta burst stimulation (*grey bar)* in naïve and ELS condition. **(i)** Bar chart comparing fEPSP slope at 30-40min post theta burst stimulation in naïve and ELS conditions.

Figure 2. Impact of ELS on astrocytes.
(a) Widefield image of GFAP, Cx43, and DAPI staining in the mouse brain, highlighting amygdala brain regions. **(b)** Confocal z-stack of the same image in the lateral amygdala. *top* single channel images of GFAP, Cx43, and DAPI with merge *below*. **(c)** Comparison of GFAP staining in naïve and ELS (normalised). **(d)** Comparison of Cx43 expression in naïve and ELS conditions (normalised). **(e)** Comparison of GLT-1 expression in naïve and ELS conditions (normalised).

Figure 3. Astrocyte dysfunction alone mirrors effects of ELS on behaviour and synapses.
(a) ***left*** Schematic representation of bilateral injection of AAVs targeting astrocyte function. ***right*** Example of fluorescent reporter expression in the lateral amygdala following AAV injection. **(b)** Three constructs were independently injected into LA to target astrocytes, (i) dnCx43, (ii) CalEx, and (ii) control virus. **(c)** Performance of dnCx43 injected mice during acquisition phase. **(d)** memory recall in dnCx43 injected mice. **(e)** Performance of CalEx injected mice in acquisition phase. **(f)** Memory recall in CalEx mice. **(g)** Comparison of discrimination index between dnCx43, CalEx, and Viral control. **(h)** Normalised fEPSP slope over the course of LTP experiment in dnCx43 and CalEx conditions. **(i)** Bar chart comparing fEPSP slope at 30-40min post theta burst stimulation in Control (eGFP), dnCx43, and CalEx injected conditions.

Figure 4. ELS increases blood glucocorticoid levels and translocation of GRs to the nucleus of astrocytes.
(a) Timeline depicting times at which mice were sacrificed and blood was taken for CORT assay. **(b)** Serum corticosterone is significantly increased during adolescence (P45) only, in ELS compared to naïve mice. **(c)** Representative confocal image showing GR immunostaining in astrocytes. Scale bars=20µm. **(d)** Relative expression of GR in the nucleus compared to cytosol was increased in ELS mice.

Figure 5. Targeting astrocyte GRs rescues effects of ELS.
(a) Schematic of lateral amygdala-specific deletion of GR in astrocytes. **(b)** *top row* -Immunostaining of viral infected astrocyte expressing cre-recombinase (and eGFP reporter), S100B confirmation of cell identity, DAPI, GR, and merge of channels. *Bottom row* shows within-brain nearby non-infected

astrocyte, lacking eGFP reporter. Scale bars=10μm. **(c)** Quantification of nuclear-GR fluorescence intensity in eGFP negative (control) and eGFP positive (GR KO) astrocytes. **(d)** Timeline highlighting viral injection post-stress, i.e. rescue experiment. **(e)** Comparison of freezing to CS+/US and CS- in ELS (green, grey) and ELS with GR KO in astrocytes (yellow, black). **(f)** Comparison of discrimination between CS+ and CS- during memory recall phase in ELS and ELS with astrocyte GR KO mice. **(g)** Discrimination index is greatly improved with astrocyte GR deletion. **(h)** Normalised field EPSP slope showing synaptic response to theta burst stimulation in ELS and ELS with astrocyte GR KO. **(i)** Bar chart showing normalised fEPSP slope at 30-40min post theta burst stimulation in naïve, ELS, and ELS with astrocyte GR KO.

Supplementary figure 1
(a) Learning phase (conditioning) of auditory discriminative fear conditioning in naïve mice. **(b)** Memory recall in of CS+ and CS- in naïve mice. **(c)** Auditory discrimination in naïve mice. **(d)** Comparison of performance in conditioning phase between female and male mice. **(e)** Comparison of performance in memory recall phase between female and male mice. **(f)** No difference in auditory discrimination between naïve female and naïve male mice. **(g)** ELS impairs auditory discrimination more strongly in female mice.

Supplementary figure 2
(a) No effect of astrocyte manipulation on time spent in open arms of EPM. **(b)** No effect of astrocyte manipulation on open arm/closed arm duration in EPM. **(c)** No effect of astrocyte manipulation on distance travelled in EPM. **(d)** No effect of astrocyte manipulation on average moving speed in EPM. **(e)** No effect of astrocyte manipulation time in centre of OFT. **(f)** No effect of astrocyte manipulation on centre/periphery duration in OFT. **(g)** Distance travelled in OFT was reduced by CalEx compared to viral control. **(h)** Average speed of locomotion in OFT was reduced by CalEx compared to viral control. **(j)** dnCx43 expression in lateral amygdala astrocytes had a stronger influence on male compared to female mice. **(k)** CalEx expression in lateral amygdala astrocytes had a stronger influence on female compared to male mice.

Supplementary figure 3
(a) Cre-eGFP expression was predominantly expressed in S100B expressing cells (astrocytes). **(b)** The rescue effect of GR KO in lateral amygdala astrocytes worked equally in female and male mice.